Journal of Chromatography A, 1217 (2010) 6405–6412

Contents lists available at ScienceDirect

Journal of Chromatography A

journal homepage: www.elsevier.com/locate/chroma

Simple capillary flow porometer for characterization of capillary columns containing packed and monolithic beds

Yan Fang[a], H. Dennis Tolley[b], Milton L. Lee[a,*]

[a] Department of Chemistry and Biochemistry, Brigham Young University, Provo, UT 84602, USA
[b] Department of Statistics, Brigham Young University, Provo, UT 84602, USA

ARTICLE INFO

Article history:
Received 29 April 2010
Received in revised form 2 August 2010
Accepted 9 August 2010
Available online 13 August 2010

Keywords:
Liquid chromatography
Capillary columns
Monolithic columns
Pore size characterization
Permeability
Capillary flow porometry

ABSTRACT

A simple capillary flow porometer (CFP) was assembled for through-pore structure characterization of monolithic capillary liquid chromatography columns in their original chromatographic forms. Determination of differential pressures and flow rates through dry and wet short capillary segments provided necessary information to determine the mean diameters and size distributions of the through-pores. The mean through-pore diameters of three capillary columns packed with 3, 5, and 7 μm spherical silica particles were determined to be 0.5, 1.0 and 1.4 μm, with distributions ranging from 0.1 to 0.7, 0.3 to 1.1 and 0.4 to 2.6 μm, respectively. Similarly, the mean through-pore diameters and size distributions of silica monoliths fabricated via phase separation by polymerization of tetramethoxysilane (TMOS) in the presence of poly(ethylene glycol) (PEG) verified that a greater number of through-pores with small diameters were prepared in columns with higher PEG content in the prepolymer mixture. The CFP system was also used to study the effects of column inner diameter and length on through-pore properties of polymeric monolithic columns. Typical monoliths based on butyl methacrylate (BMA) and poly(ethylene glycol) diacrylate (PEGDA) in capillary columns with different inner diameters (i.e., 50–250 μm) and lengths (i.e., 1.5–3.0 cm) were characterized. The results indicate that varying the inner diameter and/or the length of the column had little effect on the through-pore properties. Therefore, the through-pores are highly interconnected and their determination by CFP is independent of capillary length.

1. Introduction

The morphologies and pore structures of porous media are important in the design of chromatographic columns due to their influence on hydrodynamic properties (e.g., flow properties), thermodynamic properties (e.g., loadability) and mass transfer kinetics (e.g., efficiency). There are two classes of traditional methods for determining pore size and morphology. Microscopic techniques, such as scanning electron microscopy (SEM) and X-ray analysis, provide actual images of the surface, but no quantitative characterization of the surface area and pore volume. They are also quite involved, time consuming and expensive. However, bulk measurement techniques, such as nitrogen sorption porosimetry (BET) and mercury intrusion porosimetry (MIP) used together can rapidly and inexpensively determine the micro- to macro-porosities of materials. SEM, MIP, BET and inverse size-exclusion chromatography (ISEC) are four traditional methods for pore size characterization of packed and monolithic columns, which have been used for decades [1,2]. Newer techniques, such as atomic force microscopy (AFM) [3], transmission electron microscopy (TEM) [4], total pore blocking (TPB) [5] and, most recently, confocal laser scanning microscopy (CLSM) [6] have been used to determine pore characteristics of packed and monolithic columns. CLSM is unique in that analysis based on quantitative physical reconstruction can be used to derive the complete three-dimensional macropore morphology of monoliths.

A major question associated with the most popular methods for pore structure characterization, such as MIP and BET, is how relevant the determined pore size properties are to the chromatographic performance of the columns, especially since the measurements are made on representative bulk materials not in a column format. While ISEC can be used to obtain three-dimensional porosity properties of packed or monolithic columns in their chromatographic forms, ISEC conditions can destroy the columns, such as the use of THF as mobile phase in the polymeric monoliths reported in this paper. Furthermore, there is limited availability of appropriate standards. Recently, intraparticle Donnan-exclusion was used to determine the interparticle void space of packed beds and the interskeleton macropore space of monoliths [7]. Compared with ISEC, this is much easier to conduct,

* Corresponding author at: Brigham Young University, Department of Chemistry and Biochemistry, Provo, UT 84602-5700, USA.
Tel.: +1 801 422 2135; fax: +1 801 422 0157.
E-mail address: milton_lee@byu.edu (M.L. Lee).

0021-9673/$ – see front matter © 2010 Elsevier B.V. All rights reserved.
doi:10.1016/j.chroma.2010.08.026

since it requires no standards and can be run in convenient (HPLC) mobile phases.

Capillary flow porometry (CFP) is basically an extrusion method, and was developed for the evaluation of through-pore structure characteristics of filter materials, such as membranes, textile materials, ceramic components, and filtration media [8–19]. Using CFP, a sample is thoroughly wetted before testing. Gas flow through the sample is measured at specific pressures using a rotameter. The relationship between pressure and gas flow rate provides through-pore structure characteristics of the sample. Through-pore sizes are typically reported as pore diameters. This is straightforward for pores with circular cross-sections. Pores with irregular cross-sections are defined according to the diameter of a circular opening whose perimeter to area ratio is a circular pore at the same location [20]. That is,

$$\left(\frac{\text{perimeter}}{\text{area}}\right)_{\text{pore}} = \left(\frac{\text{perimeter}}{\text{area}}\right)_{\text{circle of diameter } d} \quad (1)$$

A key factor in the CFP technique is the selection of wetting liquid. A good wetting liquid should wet the surface of the porous materials spontaneously and possess relatively low surface tension. A wetting liquid can spontaneously fill pores but cannot flow along the surface spontaneously due to surface tension. To remove the wetting liquid from the pores, work must be done to increase the liquid/solid surface free energy. That is,

$$P\ \mathrm{d}V = (\gamma_{\text{solid/gas}} - \gamma_{\text{solid/liquid}})\mathrm{d}S \quad (2)$$

where P is the differential pressure, dV is the increase in volume of gas in the pores, γ is the surface tension, and dS is the increase in solid/gas interfacial area and corresponding decrease in solid/liquid interfacial area. If a gas is used to displace the liquid from the pores, one can show that the needed pressure for the gas to flow through the pores is given by [8]

$$P = \frac{4\gamma(\cos\ \theta)}{d} \quad (3)$$

where θ is the contact angle and d is the pore diameter. For low surface tension wetting liquids, θ can be taken as zero. Based on Eq. (3), the largest pores will be purged at the lowest pressure, while the smallest pores require the highest pressure.

Basically, CFP detects the presence of a through-pore when gas flows through that pore, which happens only when the pressure is high enough to displace the wetting liquid from the most constricted part of the pore. Consequently, the pore diameter calculated from the pressure [i.e., Eq. (3)] is the diameter of the pore at its most constricted point. Based on measurements of differential pressures and flow rates through wet and dry samples, through-pore characteristics can be computed. Since the data used are based on flow rate, characterization of the through-pore structures of chromatographic columns in their actual forms can be achieved, which makes CFP an attractive technique.

In this work, we designed and constructed a capillary flow porometer for through-pore size characterization of capillary columns. Three packed columns containing different sizes of silica particles, three silica monolithic columns and several typical polymeric monoliths based on butyl methacrylate (BMA) and poly(ethylene glycol) diacrylate (PEGDA) in capillary columns with different inner diameters (i.e., 50–250 μm) and lengths (i.e., 1.5–3.0 cm) were characterized.

2. Experimental

2.1. Sample preparation

2.1.1. Silica particle packed columns

A high pressure packing system was used for packing columns [21]. Briefly, a Model DSF-150-C1 air-driven pneumatic amplifier pump (Haskel, Burbank, CA, USA) was used to drive the packing slurry through the column. One end of a 150 μm i.d. fused silica capillary was connected to a VICI Valco 1/16″ union (VICI Valco, Houston, TX, USA) with a section of PEEK tubing (Upchurch, Oak Harbor, WA, USA) and a stainless steel frit (0.5 μm pore size) (Upchurch) to retain the particles in the capillary. The other end of the capillary was connected to a modified Swagelok reducing union, which acted as the packing material reservoir, and was connected to the Haskel pump via 1/8″ o.d. tubing.

Slurries of silica particles were made by mixing approximately 30 mg (more than enough for packing) of 3, 5 or 7 μm diameter silica particles in 200 μL of isopropanol. Then the slurry was transferred to the packing reservoir. Liquid carbon dioxide from the pneumatic amplifier pump was used to drive the silica particle slurry into the capillary column. Particles were held by the stainless steel frit in the column during packing. Both the column and the reservoir were placed in an ultrasonic bath (Branson Ultrasonic, Danbury, CT, USA) that was set at room temperature and turned on from the beginning until the column was completely filled. The pump pressure was gradually increased to 5000 psi for packing of the 7 μm particles and up to 10,000 psi for the 3 μm particles to maintain a constant filling rate. The filling process required approximately 2 h, however, each column was left overnight to depressurize [21]. After packing, frits were sintered at both ends of the columns using a capillary burner (Innova Tech, Ellicott City, MD, USA).

2.1.2. Silica monolithic columns

Silica monolithic columns were prepared as described by Motokawa et al. [22]. Before preparation, 50 μm i.d. fused silica capillary tubes (Polymicro, Phoenix, AZ, USA) were pretreated with 1 mol/L NaOH solution at 40 °C for 3 h, washed with water and acetone, and then dried. Tetramethoxysilane (TMOS, Aldrich, St. Louis, MO, USA) was added to a solution of poly(ethylene glycol) (PEG, M_W = 10,000, Sigma, St. Louis, MO, USA) and urea in 0.01 M acetic acid and stirred at 0 °C for 45 min. The resulting homogeneous solution was introduced into the pretreated fused silica capillary tube, and allowed to react at 40 °C. Gelation occured within 2 h and the gel was subsequently aged overnight at the same temperature. Then the silica monolithic column was treated at a higher temperature (120 °C) for 3 h to complete mesopore formation from ammonia generated by the hydrolysis of urea, followed by washing with water and methanol. After drying, heat-treatment was carried out at 330 °C for 25 h, resulting in decomposition of organic moieties in the capillary. Table 1 lists the reagent mixture compositions and temperatures for experimental columns A, B, and C.

2.1.3. Bulk silica monoliths

Three bulk silica monolithic samples representing each capillary sample A, B and C were prepared. Briefly, a bulk sample was

Table 1
Reagent composition and reaction temperature for the preparation of monolithic silica columns.

Column	PEG (g)	TMOS (mL)	Urea (g)	AcOH (mL)	Temp. (°C)
A	8.8	40	9.0	100	40
B	12.4	40	9.0	100	30
C	12.8	40	9.0	100	30

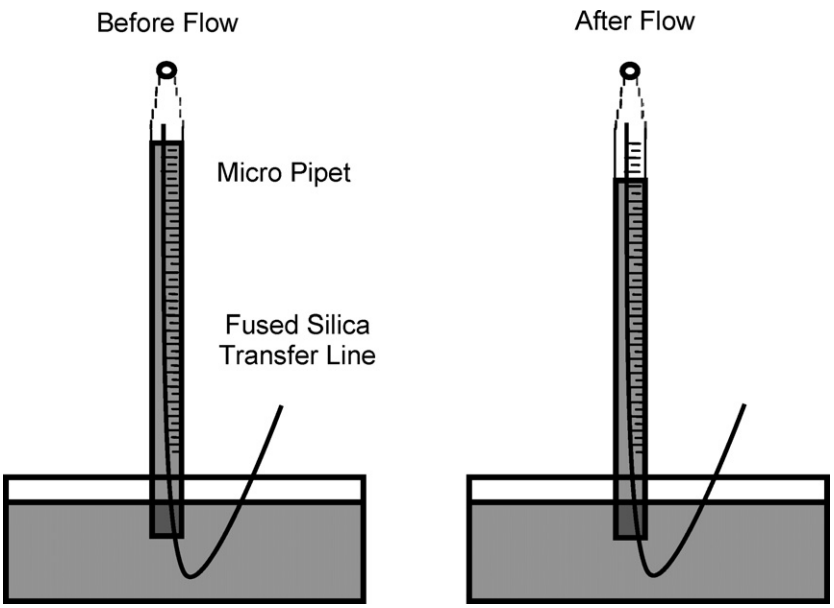

Fig. 1. Schematic of the home-built microflow meter.

prepared in a small 5 mL glass vial, transferred to a 10 mL Soxhlet thimble, placed in a Soxhlet apparatus to extract with methanol for 12 h, and finally vacuum-dried for 5 h at 60 °C.

2.1.4. Polymeric monolithic columns

Before synthesis of a polymeric monolith, the surface of the UV transparent capillary was functionalized by flushing the column first with ethanol and deionized water, followed by incubating with 2 M hydrochloric acid for 3 h at 110 °C in a GC oven. Then it was rinsed with ethanol and dried with N_2 at 110 °C overnight in a gas chromatographic (GC) oven. Afterwards, a 15% solution of 3-(trimethoxysilyl)propylmethacrylate in dried toluene was placed in the capillary overnight at room temperature. After reaction, it was rinsed with toluene and acetone and dried with N_2 overnight in the GC oven.

A prepolymer mixture of 23.9% GMA, 15.9% PEGDA, 0.40% DMPA (2,2-dimethoxy-2-phenyl-acetophenone), 4.98% methanol and 54.8% cyclohexanol, was made by weighing each ingredient based on concentration in a 5 mL glass vial. This solution was degassed for approximately 30 s to a clear solution and then introduced into the treated capillary by capillary action, followed by exposure to UV light with a cold mirror for approximately 15 min for polymerization. After reaction, the capillary column was flushed with methanol followed by deionized water using a syringe pump to finally open the pores in the skeletal structure of the monolith.

In this work, polymeric monoliths were fabricated in 50, 75, 150 and 250 μm i.d. UV transparent capillary columns to study the effect of inner diameter on pore structure. The same monolith was prepared in 75 μm i.d. capillaries in lengths of 1.5, 2.0 and 3.0 cm to explore the effect of length on the pore properties of the columns.

2.2. Scanning electron microscopy

The morphologies of the packed columns, silica and polymeric monolithic columns and bulk silica monoliths were visualized using a scanning electron microscope (FEI Philips XL30 ESEM FEG, Hillsboro, OR, USA). A small section (2 cm) of each capillary column was cut and the cross-sectional area was scanned. A section of the bulk monolith was placed on a mold and its surface was scanned.

2.3. Capillary flow porometry

A home-built gas flow meter was designed to measure the microflow rates generated during the experiments. As shown in Fig. 1, the flow meter was made from a small graduated pipette. The small end of the pipette was sealed using a high temperature flame, and the sealed pipette was filled with water and inverted with the open end submerged in a dish containing water. A 50 cm × 530 μm i.d fused silica capillary was connected at one end to a nitrogen gas source. The other end of the capillary was inserted into the open end of the seated pipette. A stop watch was used to time the displacement of water in the pipette in order to calculate the gas flow rate.

Pressure control was provided by using a digital pressure controller (Alicat Scientific, Tucson, AZ, USA). The pressure was controlled accurately (±0.25%). One end of the sample was connected to the output port of the pressure controller, while the other end was connected to the fused silica capillary inserted in the inverted pipette. When pressure was applied, the gas flow rates through the dry and wet samples were measured using the home-built microflow meter.

The dry up/wet up measurement method was applied in this work, which means that a dry curve was determined with the pressure increasing followed by a wet curve with the pressure increasing. Galwick, an oxidized, polymerized 1,1,2,3,3,3-hexafluoropropene, was used as the wetting liquid for constructing the wet curves in this study because it is widely used in CFP measurements of filters due to its very low surface tension (15.9 dynes/cm). Generally, the dry curve was measured first by increasing the nitrogen gas pressure at specific pre-set points through a 1.5 cm long dry sample. The sample was then filled with Galwick by purging with the liquid for approximate 0.5 h using a syringe pump (Harvard Apparatus, Holliston, MA, USA) at a rate of 0.1 μL/min. After the sample was thoroughly wetted, the wet curve was obtained by measuring nitrogen gas flow rate through the sample as the pressure was increased. Typically, to obtain a stable flow rate (i.e., when the pores at a specific pressure are completely cleared of the wetting liquid), approximately 20 h was required for the first applied pressure. This was because the gas flow rate was very low and only a small number of through-pores were opened. However, at higher pressure when more through-pores

Table 2
Repetitions for CFP determination of packed and monolithic capillary columns.

Column type	Column					
	1		2		3	
Particle packed columns[a]	Dry[d]	Wet[e]	Dry[d]	Wet[e]	Dry[d]	Wet[e]
3	3/1	1/3	3/1	1/3	3/1	1/3
5	3/1	1/3	3/1	1/3	3/1	1/3
7	3/1	1/3	3/1	1/3	3/1	1/3
Silica monolithic columns						
50[b] (A)	3/1	1/3	3/1	1/3	3/1	1/3
50[b] (B)	3/1	1/3	3/1	1/3	3/1	1/3
50[b] (C)	3/1	1/3	3/1	1/3	3/1	1/3
Polymeric monolithic columns[b]						
50	3/1	1/3	3/1	1/3	3/1	1/3
75	3/1	1/3	3/1	1/3	3/1	1/3
150	3/1	1/3	3/1	1/3	3/1	1/3
250	3/1	1/3	3/1	1/3	3/1	1/3
Polymeric monolithic Columns[c]						
1.5	3/1	1/3	3/1	1/3	3/1	1/3
2.0	3/1	1/3	3/1	1/3	3/1	1/3
3.0	3/1	1/3	3/1	1/3	3/1	1/3

[a] Particle diameter (μm).
[b] Column internal diameter (μm).
[c] Column length (cm).
[d] 3 determinations (i.e., 3 replications) of the total curve with 1 measurement of flow for each set pressure.
[e] 1 determination of the total curve with 3 measurements (i.e., 3 replications) of flow for each set pressure.

were opened, the equilibration time could be as short as several minutes. Table 2 lists the repetitions of measurements made for the dry and wet curves for all of the capillary columns tested. For the dry curves, three replications of each curve was made with only one measurement at each set pressure. For the wet curves, a single replication (only one curve) was made with three repeated measurements at each set pressure (see footnotes to Table 2).

The mean through-pore diameter and pore size distribution were determined. The largest pore diameter is indicated when the first gas bubbles start to form from a sample as the pressure is increased. This occurs when the wet curve deviates from the *x*-axis.

The distribution of through-pore sizes gives the relative proportion of through-pores of each size. From Eq. (3) we see that for a particular through-pore, the "size" is the diameter at the most constricted point of the pathway described by the through-pore (i.e., throat pore diameter). This diameter is determined by the amount of work necessary to push the wetting liquid through the pore.

The relative proportion of through-pores of a particular diameter is measured by comparing the flow rate through the capillary at the pressure associated with the specific diameter relative to the flow rate under dry conditions at that same pressure [9,11]. If there is only one through-pore at a specific diameter, then the wetting agent will clear at the appropriate pressure, as given by Eq. (3). However, an increase in flow rate with the opening of a single pore will be nominal. If, however, there are many through-pores of this diameter, the increase in flow rate will be larger. Thus, the determination of the relative proportion entails determining the proportion of through-pores that are cleared of wetting agent at each specific pressure. Using Eq. (3), we can determine the diameter for each specific pressure.

The relative flow rate is determined by comparing the flow rate under wet conditions with those under dry conditions. Specifically, the filter flow for CFP is defined as [19]

$$\text{Filter flow\% (FF\%)} = 100 \times \frac{\text{wet flow}}{\text{dry flow}} \quad (4)$$

Table 3
CFP determination of mean through-pore diameters compared to calculated through-pore diameters for packed capillary columns.

Particle diameter (μm)	Column mean pore diameter (μm)			Average	RSD (%)	Calculated[a] (μm)
	1	2	3			
3	0.52	0.48	0.55	0.52	6.75	0.68
5	1.04	1.02	0.96	1.01	4.12	1.13
7	1.45	1.35	1.40	1.40	3.33	1.59

[a] Calculated from close-packed arrangement.

From this, the incremental flow is

$$\text{Incremental filter flow\% } (\Delta\text{FF\%}) = \text{current FF\%} - \text{previous FF\%} \quad (5)$$

$$\text{Incremental pore diameter } (\Delta d) = \text{previous diameter} - \text{current diameter} \quad (6)$$

The through-pore distribution is thus the increase in incremental flow relative to the increase in diameter [9,11]:

$$\text{Relative pore size distribution portion} = \frac{\Delta\text{FF\%}}{\Delta d} \quad (7)$$

The diameters are calculated using Eq. (3). The value for each diameter pore interval corresponds to the pore size distribution for that interval:

$$\text{Mean diameter} = \frac{1}{2}(\text{previous diameter} + \text{current diameter}) \quad (8)$$

3. Results and discussion

3.1. Through-pore size characterization of silica particle packed columns

CFP measures the gas flow rate through dry/wet monoliths at specific differential pressures. The relationship between gas flow rate and differential pressure, called the dry/wet curve, can be obtained in sequence. The through-pore diameter is calculated from the differential pressure according to Eq. (3). Although each pore may have a range of diameters, CFP only measures the most constricted part, which is called the throat pore diameter. Based on the definition of the dry curve, the half-dry curve is half of the gas flow rate through the dry sample as a function of differential pressure. The pressure where the wet and half-dry curves intersect gives the mean through-pore diameter as defined by ASTM standard method F316-86. While flow through the mesopores cannot be excluded for the dry curve compared to the wet curve, the contribution to the total flow is expected to be minimal.

Fig. 2 shows representative wet, dry, and half-dry curves for packed columns containing 3, 5 and 7 μm diameter silica particles determined by CFP. At a specific differential pressure, the gas flow rate through a wet sample is always smaller than that through the corresponding dry sample until finally the two curves meet together, when all wetting liquid in the through-pores is purged out of the sample.

Table 3 summarizes the mean through-pore diameters obtained from CFP for packed columns containing 3, 5 and 7 μm particles: 0.5 ± 0.02, 1.0 ± 0.17, and 1.4 ± 0.01 μm, respectively. Theoretical equivalent diameters from a close-packed arrangement were calculated from simple geometry of three identical particles touching each other in a planar two-dimensional arrangement. The measured values were all smaller than the equivalent calculated through-pore diameters (i.e., 0.7, 1.1 and 1.6 μm). This difference is most likely due to the combined effect of three causes: (1) sintering of packing materials at both ends of the columns to retain

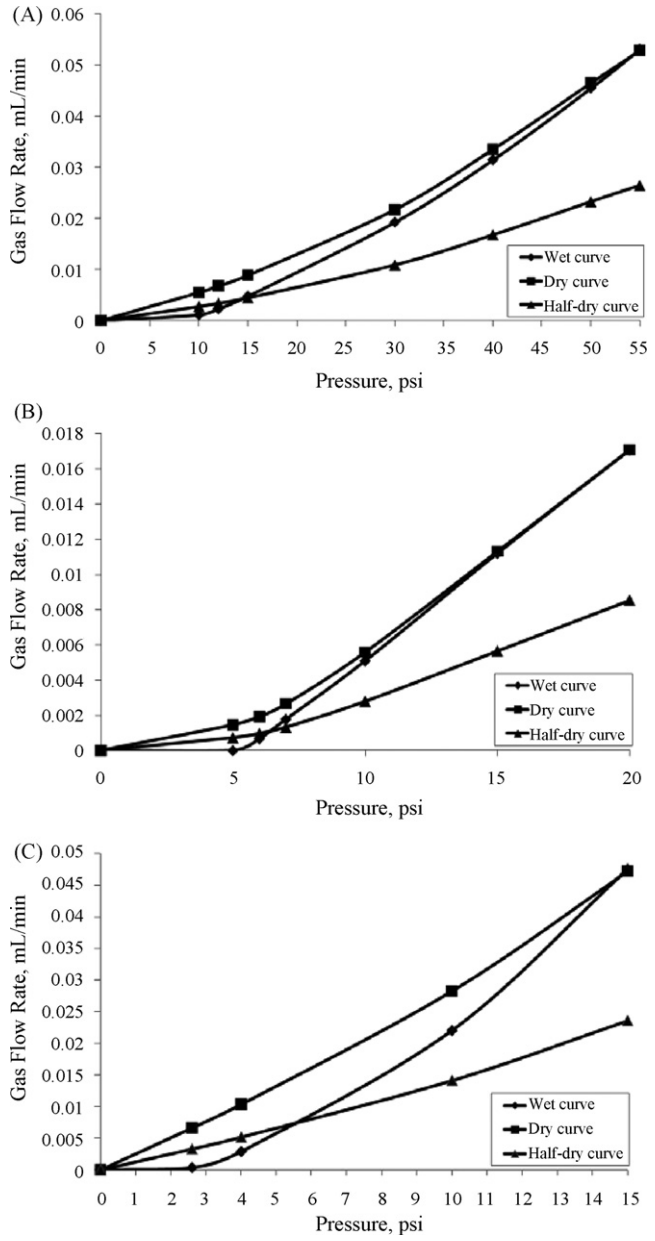

Fig. 2. Wet, dry and half-dry curves for packed capillary columns containing (A) 3, (B) 5 and (C) 7 μm diameter particles measured using CFP.

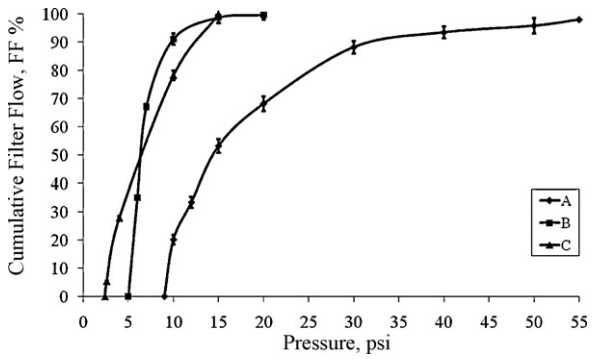

Fig. 3. Cumulative filter flows for capillary columns packed with (A) 3, (B) 5 and (C) 7 μm particles measured using CFP.

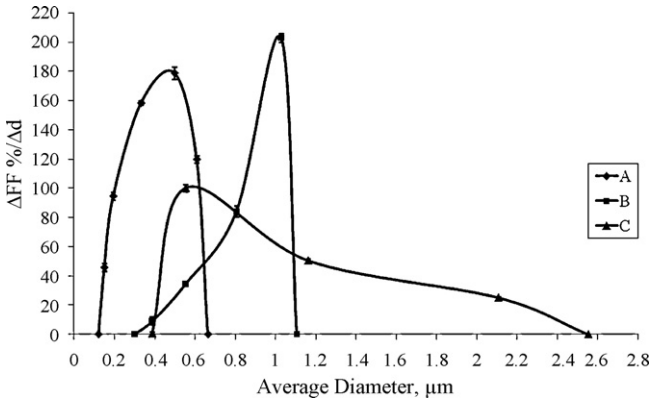

Fig. 4. Through-pore size distributions for capillary columns packed with (A) 3, (B) 5 and (C) 7 μm particles determined by CFP.

the particles inside the capillary, (2) presence of a significant percentage of small particles in a wide particle distribution, and (3) the fact that most of the pressure drop occurs at the end of the column. All of these would result in smaller measured mean pore diameters because CFP only detects the most constricted part of a through-pore diameter.

Fig. 3 shows representative cumulative filter flows for columns packed with 3, 5 and 7 μm particles as determined using CFP. It is evident that all samples finally reached 100% cumulative filter flow. However, the minimum pressure to empty all through-pores in a column depended on the specific column through-pore characteristics. Due to its very large through-pores, the column packed with 7 μm particles only required 15 psi gas pressure to purge all of the wetting liquid from its pores, while 20 and 55 psi gas pressures, respectively, were required for columns packed with 5 and 3 μm particles.

Fig. 4 shows representative curves of the through-pore size distributions for columns packed with 3, 5 and 7 μm particles as determined by CFP. The area under the distribution curve in any pore size range is the percentage flow in that range. The representative through-pore size distributions indicate that for 7 μm diameter silica particles, the pores were distributed in a broad range of 0.4–2.6 μm. However, for 5 and 3 μm diameter silica particles, the pore size ranges shifted to much smaller values, i.e., 0.3–1.1 and 0.1–0.7 μm, respectively. Because the particle sizes are not completely uniform (as observed from SEM images of the particles), we found some smaller pores in the column packed with 7 μm particles and some larger pores in the column packed with 5 μm particles (also qualitatively observed from SEM images of the columns).

3.2. Through-pore size characterization of silica monolithic columns

The mean through-pore diameters of silica monoliths A, B and C as listed in Table 4 were sequentially smaller due to an increase in concentration of PEG in the prepolymer mixture. This was initially observed from SEM images and subsequently verified using CFP. The cross-over points of the wet and half-dry curves gave the mean through-pore diameters of columns A, B and C as 3.9, 1.3 and 0.8 μm (Table 4), respectively, which strongly support the former conclusion regarding the concentration of PEG. Fig. 5 shows representative

Table 4
CFP determination of mean through-pore diameters for silica monolithic capillary columns.

Column	Mean pore diameter (μm)			Average	RSD (%)
	1	2	3		
A	3.92	3.84	3.95	3.90	1.46
B	1.27	1.36	1.30	1.31	3.78
C	0.81	0.83	0.77	0.80	4.25

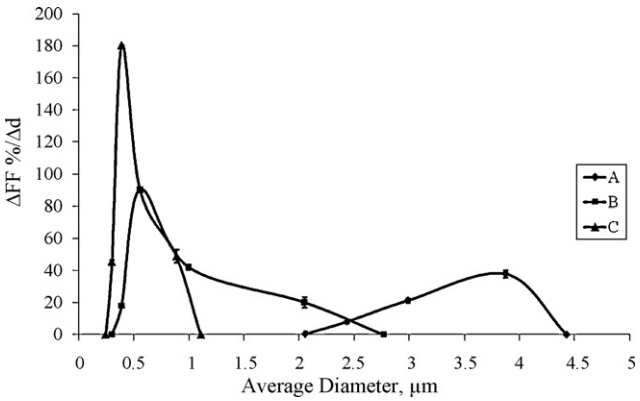

Fig. 5. Through-pore size distributions for silica monolithic capillary columns A, B, and C determined by CFP.

curves of the through-pore size distributions for monoliths A, B and C. Most through-pores in monolith A were between 2.1 and 4.4 μm, explaining the very low back pressure observed for this column. Some of the through-pores in column B were as large as 1.0–2.8 μm, while some were as small as 0.3 μm. Monolith C gave the smallest pores and narrowest pore size distribution in the range of 0.2–1.1 μm.

Fig. 6 shows SEM images of monoliths A, B and C synthesized in bulk (right) and in capillaries (left). The left images qualitatively support the pore properties measured using CFP. Many reports of monolithic columns include pore size properties based on measurements of representative bulk materials with the use of MIP or BET [22–28]. However, when bulk monoliths were fabricated in small glass vials from the same solutions which were used to fabricate monoliths A, B, and C inside capillary tubes, we found that the through-pore structures were quite different. The SEM images in the left column (in capillary) and right column (in bulk) in Fig. 6 indicate that monoliths confined in capillary tubes produced larger through-pores. This could result because chemical reactions occur in different environments, which can affect conditions, such as pressure, temperature, and heat dissipation.

3.3. Through-pore size characterization of polymeric monolithic columns

SEM images of monolithic columns with inner diameters of 50, 75, 150, and 250 μm did not indicate any difference in through-pore

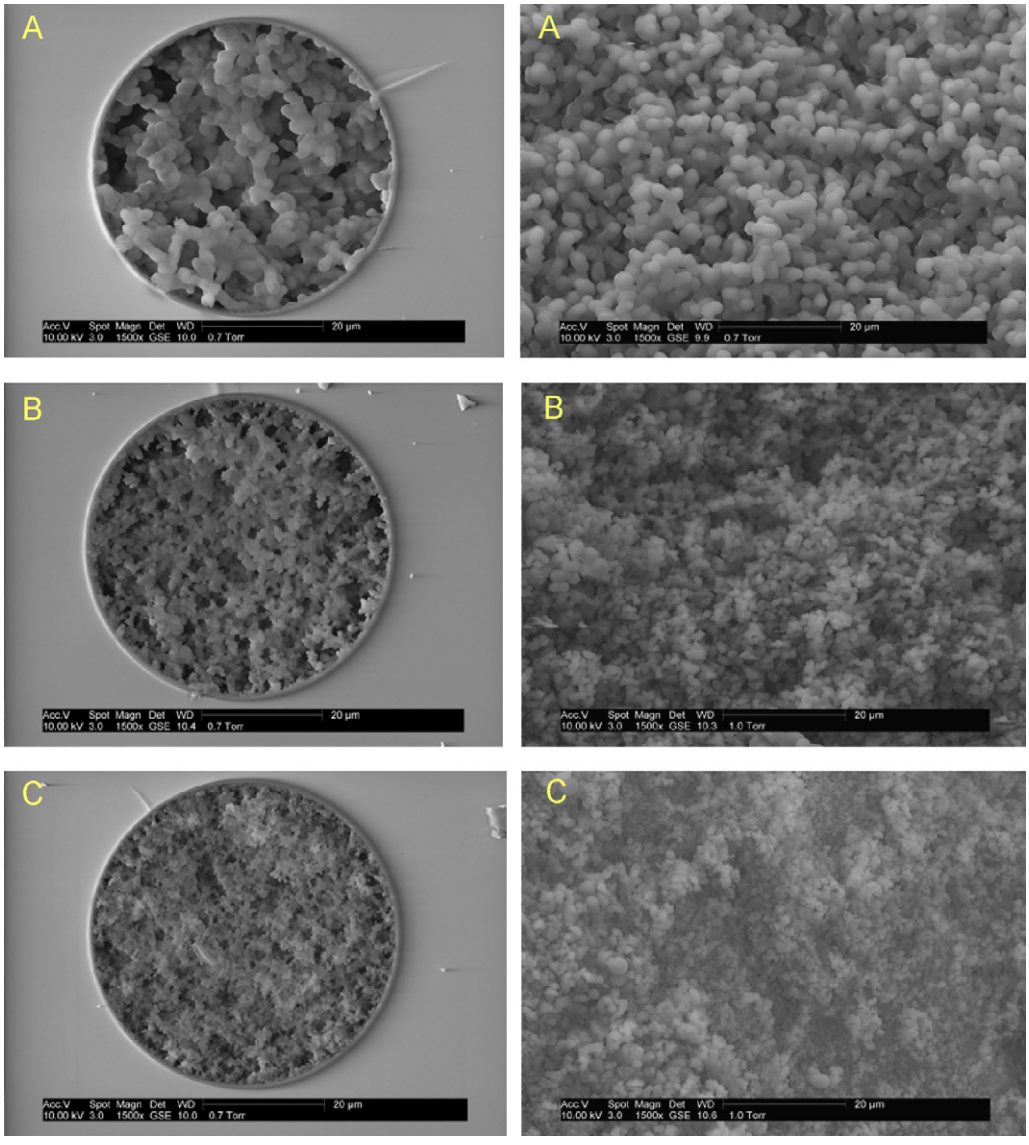

Fig. 6. SEM images of silica monoliths A, B, and C in capillaries (left) and in bulk (right) (1500× magnification).

Table 5
CFP determination of mean through-pore diameters for polymeric monolithic capillary columns.

Column i.d. (μm)	Column mean through-pore diameter (μm)			Average	RSD (%)
	1	2	3		
50	0.67	0.70	0.75	0.71	5.72
75	0.72	0.77	0.80	0.76	5.29
150	0.78	0.72	0.77	0.76	4.25
250	0.73	0.74	0.78	0.75	3.53

size. Pressures of 9.88, 9.19, 8.56 and 9.15 psi at the intersecting points of the wet and half-dry curves also indicated similar mean pore diameters for all of the columns, regardless of column inner diameter. Table 5 lists the mean through-pore diameters of the columns tested.

Studies have shown that there is only a very moderate temperature effect on through-pore size in columns with inner diameters <1 mm [29]. This can explain why a similar mean through-pore size was determined by CFP for columns with inner diameters from 50 to 250 μm. The heat generated during polymerization can be dissipated well enough in either the 50 or 250 μm i.d. capillaries. However, there should be a critical inner diameter for which the temperature effect starts to be significant. This diameter may be different for different prepolymer reagents.

Fig. 7 shows the through-pore size distributions of columns with different diameters as measured using CFP. There is very little difference in pore size distribution among these four columns. Generally, the through-pores are distributed in the range of 0.30–1.75 μm. The monolith prepared in the 50 μm i.d. capillary shows a little higher percentage of larger pores, while the monolith prepared in a 250 μm i.d. capillary has more pores with smaller diameters. Table 6 lists the relative standard deviations of the through-pore size distributions for these four columns.

In order to check the interconnectivity of through-pores in this polymeric monolithic column, and to further verify the reliability of the new CFP system, monolithic columns with lengths of 1.5, 2.0 and 3.0 cm, all with internal diameter of 75 μm, were characterized using the home-made CFP. Table 7 lists the mean through-pore diameters for these columns. Although there were differences in the wet and dry flow rates in columns of different lengths, the intersecting points of the wet and half-dry curves for the columns appeared at approximately the same differential pressure of 9.25 psi. This means that these three columns have a similar mean through-pore diameter of 0.71 μm. Furthermore, all of the dry and wet curves converged to the same differential pressure, 25 psi, corresponding to a through-pore diameter of 0.27 μm, which is the smallest through-pore size detectable in this monolith using CFP.

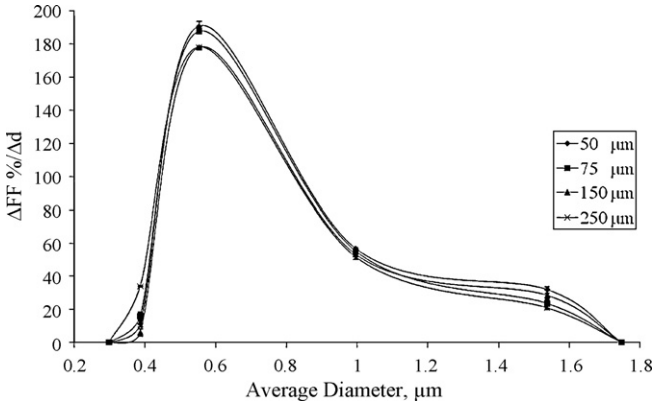

Fig. 7. Through-pore size distributions for polymeric monolithic capillary columns prepared in 50, 75, 150 and 250 μm i.d. capillaries determined by CFP.

Table 6
Through-pore size distributions for different i.d. polymeric monolithic capillary columns.

Set pressure (psi)	Calculated through-pore diameter (μm)[a]	ΔFF %/Δ*d*				RSD (%)
		50 μm i.d.	75 μm i.d.	150 μm i.d.	250 μm i.d.	
3.8	1.75	0.00	0.00	0.00	0.00	0.00
5.0	1.54	30.2	21.3	28.7	20.0	20.5
10.0	1.00	56.2	54.6	53.5	50.1	4.82
15.0	0.55	190	189	179	178	3.47
20.0	0.39	12.7	17.5	5.17	34.1	70.6
25.0	0.30	0.01	0.05	0.01	0.04	75.0

[a] *d* is derived from the set pressure as given by Eq. (3).

Table 7
CFP determinations of mean through-pore diameters for polymeric monolithic capillary columns.

Column length (cm)	Column mean through-pore diameter (μm)			Average	RSD (%)
	1	2	3		
1.5	0.72	0.73	0.72	0.72	0.80
2.0	0.72	0.71	0.70	0.71	1.41
3.0	0.71	0.71	0.69	0.70	1.64

The through-pore size distributions for all of the columns showed remarkably similar shape and range. Even though different gas flow rates were measured for these columns, both dry and wet curves changed together, resulting in a similar ratio between the wet and dry curves at every differential pressure for all columns. Consequently, the computed through-pore size distributions for all of the columns are identical in the range of 0.30–1.75 μm. Since in most cases the three different length columns were cut from the middle sections of a longer column, the pore size distributions indicate that the through-pore morphology was consistent along the length of the column, and the through-pores were highly interconnected.

4. Conclusions

A home-built CFP system was used to characterize the through-pore sizes of silica particle packed columns, and silica and polymeric monolithic columns. The mean through-pore diameters and pore size distributions were measured. The mean through-pore diameters of the three packed columns were measured to be 0.5 ± 0.02, 1.0 ± 0.17, and 1.4 ± 0.01 μm, which are all smaller than the through-pore diameters calculated from a close-packed arrangement (i.e., 0.7, 1.1 and 1.6 μm), with distributions ranging from 0.1 to 0.7, 0.3 to 1.1 and 0.4 to 2.6 μm, respectively. These pore size distributions are a combination of smaller pore diameters in the retaining frits, relatively large fractions of smaller than specified particles in the samples as observed by SEM, and the fact that the pressure drop occurs mostly at the end of the column.

The measurements verified that the mean through-pore diameters decreased for three silica monoliths with increasing concentration of PEG in the reaction mixture. A comparison of SEM images of silica monoliths indicate that monoliths confined in capillary tubes produced larger through-pores than bulk monoliths fabricated in small glass vials from the same prepolymer solutions.

A typical polymer monolithic stationary phase based on BMA and PEGDA was synthesized for study of the effects of column inner diameter and length on monolith through-pore properties using CFP. Four columns with inner diameters of 50, 75, 150 and

250 μm were fabricated, and the 75 μm i.d. column was cut into three shorter columns with lengths of 1.5, 2.0 and 3.0 cm. The mean through-pore diameters and the pore size distributions indicated that similar through-pore structures were obtained for all columns studied. Heat generated during polymerization was easily dissipated through the capillary walls. Therefore, temperature effects were not significant.

The mean through-pore diameters and the through-pore size distributions also showed that the through-pore properties of the three polymer columns with different lengths were identical, which verified that the through-pores in the monolith were highly interconnected and the pore structures were uniform. Therefore, it is not necessary to use precise capillary lengths for CFP determinations. Most importantly, this finding validates the use of CFP for determination of monolithic through-pore sizes directly in capillary columns. This technique shows promise in evaluating the heterogeneity of actual packed and monolithic columns.

Acknowledgments

We appreciate the financial support from the National Institutes of Health, Contract No. R01 GM064547-01A1, and Berkeley HeartLab for this work.

References

[1] C. Liang, S. Dai, G. Guiochon, Anal. Chem. 75 (2003) 4904.
[2] D. Lubda, W. Lindner, M. Quaglia, C.F. Hohenesche, K.K. Unger, J. Chromatogr. A 1083 (2005) 14.
[3] J.L. Cabral, D. Bandilla, C.D. Skinner, J. Chromatogr. A 1108 (2006) 83.
[4] J. Courtois, M. Szumski, F. Georgsson, K. Irgum, Anal. Chem. 79 (2007) 335.
[5] D. Cabooter, F. Lynen, P. Sandra, G. Desmet, J. Chromatogr. A 1157 (2007) 131.
[6] D. Hlushkou, S. Bruns, U. Tallarek, J. Chromatogr. A 1217 (2010) 3674.
[7] S. Jung, S. Ehlert, M. Pattky, U. Tallarek, J. Chromatogr. A 1217 (2010) 696.
[8] V. Gupta, A. Jena, Adv. Filtr. Sep. Technol. 13b (1999) 833.
[9] A.K. Jena, K.M. Gupta, J. Power Sources 80 (1–2) (1999) 46.
[10] A.K. Jena, K.M. Gupta, Fluid/Particle Sep. J. 14 (3) (2002) 227.
[11] A. Gigova, J. Power Sources 158 (2006) 1054.
[12] A.K. Jena, K.M. Gupta, Am. Ceram. Soc. Bull. 82 (2003) 9401.
[13] H. Sanders, A.K. Jena, Ceram. Ind. 150 (2000) 26.
[14] N. Gupta, A. Jena, K. Gupta, Ceram. Ind. 151 (2001) 24.
[15] G. Rideal, Filtr. News July/August Issue (2004) 8.
[16] A. Jena, K. Gupta, INTC 10 (2000) 0.
[17] A. Jena, K. Gupta, Int. Wovens J. Summer Issue (2005) 26.
[18] E. Mayer, Filtr. News September/October Issue (2002) 12.
[19] ASTM Procedure F316-86, Standard Test Method for Pore Size Characteristics of Membrane Filters by Bubble Point and Mean Flow Pore Test, February 21, 1986.
[20] A.K. Jena, K.M. Gupta, Int. Nonwovens J. Fall (2003) 45.
[21] Y. Xiang, B. Yan, B. Yue, C.V. McNeff, P.W. Carr, M.L. Lee, J. Chromatogr. A 983 (2003) 83.
[22] M. Motokawa, H. Kobayashi, N. Ishizuka, H. Minakuchi, K. Nakanishi, H. Jinnai, K. Hosoya, T. Ikegami, N. Tanaka, J. Chromatogr. A 961 (2002) 53.
[23] G. Puy, R. Roux, C. Demesmay, J.L. Rocca, J. Iapichella, A. Galarneau, D. Brunel, J. Chromatogr. A 1160 (2007) 150.
[24] H. Yang, Q. Shi, B. Tian, S. Xie, F. Zhang, Y. Yan, B. Tu, D. Zhao, Chem. Mater. 15 (2003) 536.
[25] B. Grimes, R. Skudas, K. Unger, D. Lubda, J. Chromatogr. A 1144 (2002) 14.
[26] C. Viklund, E. Pontén, B. Glad, K. Irgum, P. Hörstedt, F. Svec, Chem. Mater. 9 (1997) 463.
[27] M. Thommes, R. Skudas, K. Unger, D. Lubda, J. Chromatogr. A 1191 (2008) 57.
[28] K. Unger, R. Skudas, M. Schulte, J. Chromatogr. A 1184 (2008) 393.
[29] F. Svec, T.B. Tennikova, Z. Deyl, Monolithic Materials: Preparation, Properties and Applications, Elsevier, Amsterdam, 2003.